

A study using F.E.A , theory and experiments for single helical piles in sand

Walaa-Eldin Elsherif Mohamed ¹
<https://orcid.org/0000-0002-5741-735>



Abstract Simple, low cost and easy to install deep foundation is the ideal solution to use in a lot of cases that needs deep foundation, so ,A complete study of helical pile will help a lot for using and spreading it's use. This study focused on A finite element analysis of helical pile with a single helix with various diameters and embedment ratio under the influence of compression, uplift and lateral forces. We aimed to build equations that help predicting bearing capacities of helical piles with the knowledge of it's diameter and depth (depth ratio). So by knowing it's diameter and it's depth we can get it's compression, uplift and lateral capacities. Plaxis results were used to make a comparison between them and either laboratory and theoretical results. Analyzing these results to extract equations that relate between lab and theoretical results, F.E and theoretical and F.E and Lab results. These equations should help designing any helical pile in sand.

Keywords: Helical Piles, Anchors, Axial load, Lateral Load.

1 Introduction

(Alexander Mitchell) Invented Helical piles to support light houses in England, steel circular or square shaft and a single, double or triple helix welded to the shaft are the main components of the helical pile. Easily By rotating its upper end we can install It, it can be used to resist compression, uplift and lateral forces. Such as all deep

foundations it transfer load of structures through the unsuitable soil layer to a stronger one. Helical piles have been used as foundation support for prune jacks, pipelines, and light structures that are subjected to large wind loads. In particular, helical piles are selected for resisting large uplifting forces associated with transmission towers, guyed towers, utility poles, and aircraft Moorings, and submerged pipelines. They can also provide structural support for excavations, tunnels and hydraulic structures. It has a lot of advantages over concrete and sand piles that it has a so light weight compared to them it can correct and supports existing foundation that have settled or failed, can be installed with no noise, no drilling output, no dewatering needed in sites that has high ground water lever, no need for huge equipment to install. The current design methods of single helical piles are based on the same framework and theories of conventional piles, where the compressive capacity of the pile is provided by a combination of shaft resistance and bearing resistance on the helix

([Mitsch and Clemence, 1985](#); [Rao, et al. 1991](#); [Zhang, 1999](#); and [Livneh and El Nagggar, 2008](#)).

- **Method Of Analysis**

- 1- **Theoretical Analysis**

Theories we used to determine Bearing Capacity of Helical Piles.

Compression Capacity:

Received: 11 March 2023/ Accepted: 27 May 2023

□Corresponding Author Name : Walaa Edlin Elsherif
, E-mail Wala2_r@mhiet.edu.eg , Wala2_r@yahoo.com

1.A Lecturer at Elminya higher institute of engineering and technology, Egypt

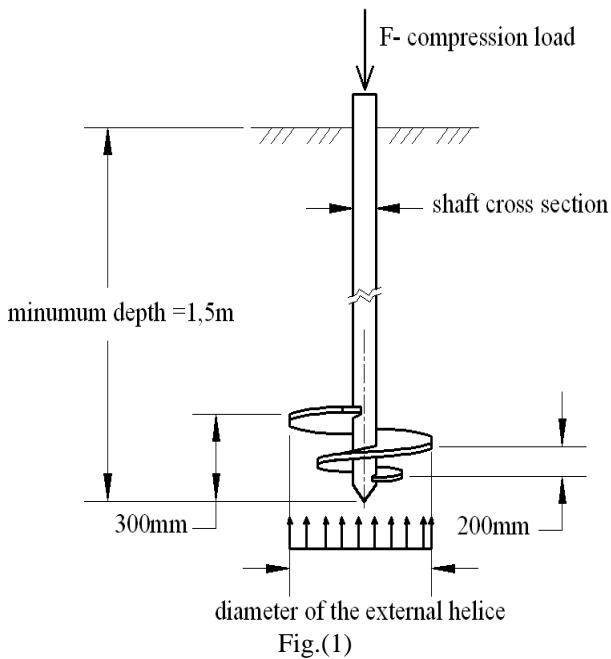


Fig.(1)

For a cohesionless soil the ultimate compression capacity of the helical screw pile using a cylindrical shearing method (Where $H/D \geq 5$) as proposed by (Mitsch and Clemence, 1985) is,

The total failure resistance can be summarized as follows, see Equation (1):

$$Q_c = Q_{helix} + Q_{bearing} + Q_{shaft} \dots \dots \dots (1)$$

where:

- Qc: ultimate pile compression capacity [t];
- Q helix: shearing resistance mobilized along the cylindrical failure surface [t] For 1 helix it's neglected;
- Q bearing: bearing capacity of pile in compression [t];
- Q shaft: resistance developed along steel shaft [t] (Mitsch and Clemence ; Narasimha et al.).

$$Q_{bearing} = \gamma' \cdot H \cdot A_H \cdot N_q \quad **$$

$$Q_{shaft} = 1/2 \cdot P_s \cdot H_{eff}^2 \cdot \gamma' \cdot K_s \cdot \tan \phi \quad **$$

So the Equation used for 1 helix is

$$Q_c = \gamma' H A N_q + 1/2 P_s H_{eff}^2 \gamma' K_s \tan \phi \quad **$$

- Qc: ultimate pile compression capacity [t];
- D: diameter of helix [m];
- Nc; Nq – dimensionless bearing capacity factors;
- D: diameter of the shaft [m];
- γ' : the volume weight [t/m³];
- Ks: coefficient of lateral earth pressure in compression loading;
- Φ : soil angle of internal friction in degrees;
- H: the embedment depth of pile [m]
- Ps: perimeter of the screw pile shaft;

Uplift Capacity :

An ultimate uplift capacity for circular Helix embedded in sand was proposed by

For a single helix helical pile, the cylindrical shearing

resistance

connecting the top and bottom helix for multi-helix piles does not

develop. Therefore, the total resistance is derived from shaft and bearing resistance (Fig. 2). Equations used to obtain axial capacity for the multi-helix helical piles should be adjusted to not include the cylindrical component.

The tension loading, Q_t in cohesionless soil for single helical piles installed in Shallow condition ($H/D \leq (H/D)_{cr}$)

$$Q_t = \gamma' \cdot H \cdot A_H \cdot F_q \quad (2)$$

The tension loading, Q_t in cohesionless soil for single helical piles installed in deep condition ($H/D > (H/D)_{cr}$)

$$Q_t = \gamma' \cdot H \cdot A_H \cdot F_q^* + 1/2 P_s \cdot H_{eff}^2 \cdot \gamma' \cdot K_u \cdot \tan \phi \quad (3)$$

Tension Loading Forces

Acting on Single Helix Helical Pile The uplift capacities for helical piles installed in cohesionless soils studied by (Mohamed Sakr 2010) estimated using

Eqn.(4), Below.

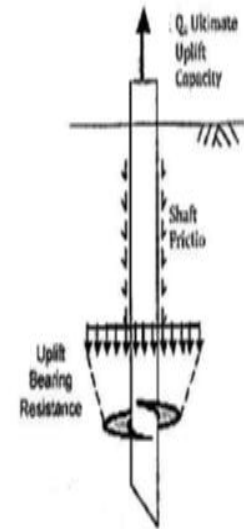


Fig.(2)

$$R = \sum Q_h + \sum Q_f \quad (4)$$

The individual helix uplift capacity, Q_h , can estimated using Eqn (5) (Das, [29]) listed below.

$$Q_h = A_h (\gamma D_h F_q) \quad (5)$$

Where:

Dh: depth to helical bearing plate

F_q : Breakout Factor.

The breakout factor, F_q , is defined as the ratio between the uplift bearing pressure and the effective vertical stress at the upper helix level. The following expression can be used to estimate the breakout factor

Lateral Capacity (Fig. 3):

Mittal et al. (2010) have developed an empirical equation for calculating the ultimate lateral load capacity of helical pile. Eq. (6)

$$Q_l / \gamma d^3 = A \times (L/d)^{2.431} \times (n^{0.2836}) \times (H_{ag}/B)^{-0.6284} \quad (6)$$

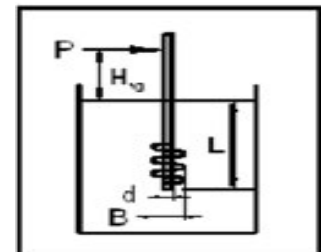


Fig.(3)

A constant from regression process ($A = 5.007$),
 Q_1 ultimate lateral load (t),
 c unit weight of soil (t/m^2),
 d diameter of pile shaft (m),
 B diameter of helical plate (m),
 L embedded length of pile (m),
 n number of helical plates, and
 H_{ag} height above ground (m).

2- Finite Element Analysis

A model of Helical Pile of different embedment ratios and diameters was analyzed using finite element analysis software Plaxis 3D for the analysis of compression, Uplift and lateral capacities

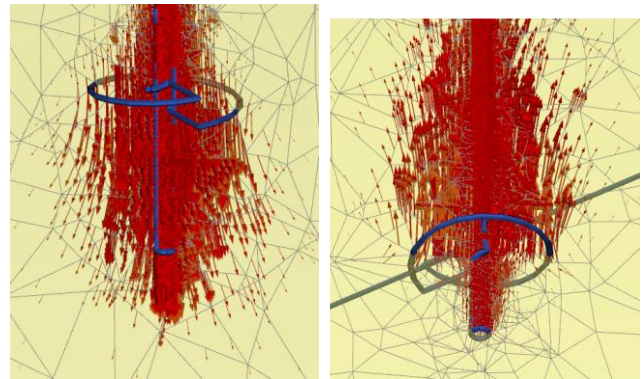
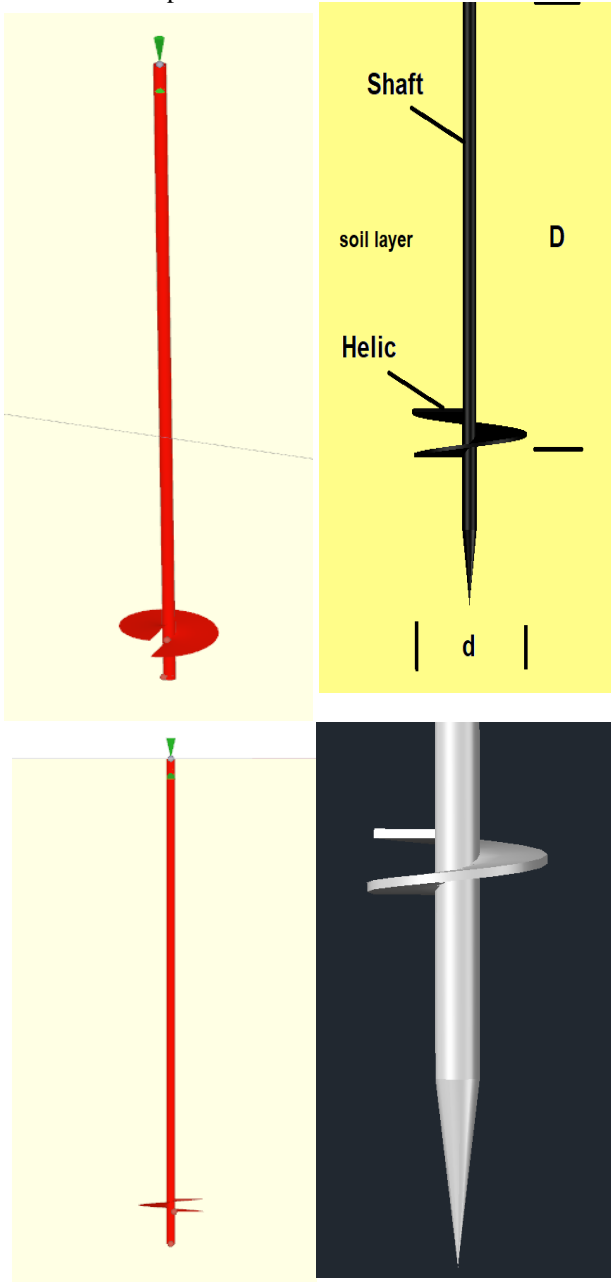
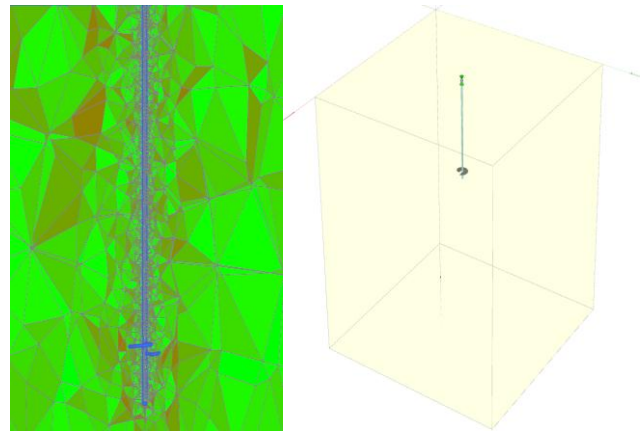


Fig.(4)

Fig.. 4 Typical helical pile model used for analysis

Soil Model:

The soil surrounding the helical pile is considered as sandy soil which extends to a depth of 1750 mm underneath the ground surface. The soil layer is modelled using borehole option in PLAXIS 3D by taking suitable plan dimensions.

The plan dimensions of soil layer are taken as 2000 mm 2000 mm and depth is kept as 1750 mm. And Medium to Fine Sand Properties was taken as (Table 1):

Properties	Symbol	Values	Units
Young's Modulus	E_{50}^{ret}	18.46×10^3	KN/m^2
	E_{ur}^{ret}	55.38×10^3	KN/m^2
Density	ρ	18	KN/m^3
Poisson's Ratio	ν	0.2	
Angle of friction	ϕ	34	Degree°
Cohesion	C	0	Kpa

Table 1

Helical pile Model

The single Helical pile is modelled in PLAXIS 3D software by poly-curve and extrude options.

The helical itself was drawn in AutoCAD 3d Application then was imported to Plaxis 3d , Helical Pile properties was taken as follow (Table 2):

Properties	Symbol	Values	Units
Young's Modulus	E	210×10 ⁶	KN/m ²
Density	ρ	75	KN/m ³
Poisson's Ratio	ν	0.15	

Table 2

Case Study

The dimensions of finite element model were selected so the boundaries are far enough to cause any restriction or strain localization to the analysis. 84 cases were analyzed in this study. the most factors affecting the distribution of load between helical piles and soil are examined. The helical diameters of helical pile was taken (5,6.7,8.2,10) cm, the helical pile embedment ratios (D/d) are taken as 1, 2, 3, 4, 5, 6 and 7 where the same sand soil in concert layer was utilized in the FEM analysis and the depth of each test was as (Table 3).

Different helix diameters and embedment ratios used was as follow

Helix Diameter	Depth At Embedment Ratio (D/d) Of							
	0	1	2	3	4	5	6	7
5	0	5	10	15	20	25	30	35
6.7	0	6.	13.	20.	26.	33.	40.	46.
		7	4	1	8	5	2	9
8.2	0	8.	16.	24.	32.	41	49.	57.
		2	4	6	8		2	4
10	0	10	20	30	40	50	60	70

Table 3

Results and Discussion

The results of this study can be divided into two parts: 1st part is F.E. Analysis of single helical pile: Pile was subjected to Compression, Uplift and lateral Forces with different diameters (5, 6.7, 8.2, 10) and different embedment ratios (1,2,3,4,5,6,7) A failure settlement criterion of 10% of the helix diameter was considered 2nd part is the comparison between F.E.A , Experimental and theoretical results

1st part Finite Element (Plaxis) Results

The results due to finite element analysis (Plaxis 3d) can be summarized and charted in Fig. (5) for compression and in Fig.(6) for uplift and for Fig. (7) for lateral capacities

Fig. (5) shows the relation between Embedment Ratio D/d and compression capacity for single helical pile with different diameters

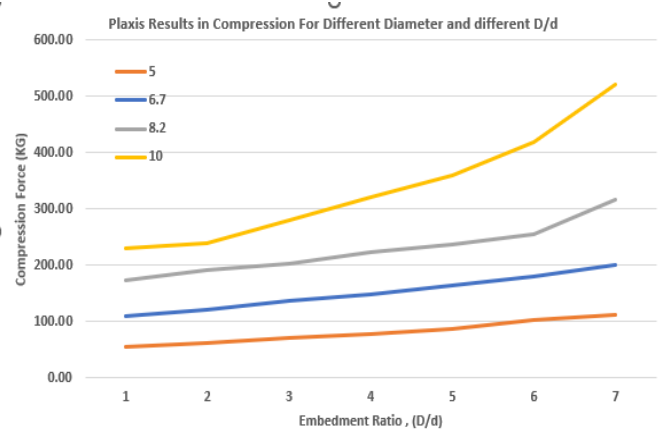


Fig. (5) compression capacity versus Embedment Ratio D/d for single helical pile with different diameters Fig. (6) shows the relation between Embedment Ratio D/d and uplift capacity for single helical pile with different diameters

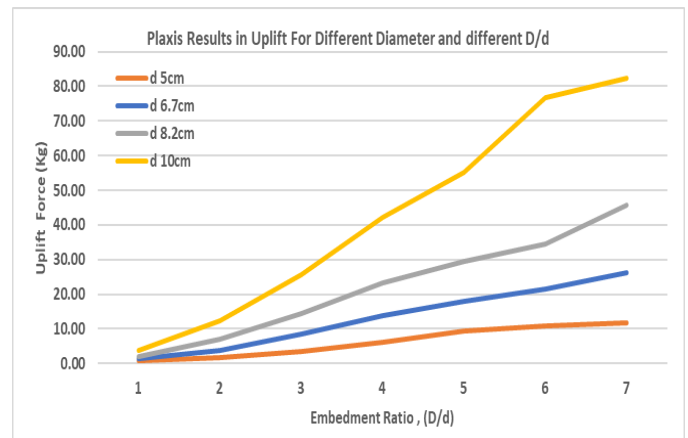


Fig. (6) uplift capacity versus Embedment Ratio D/d for single helical pile with different diameters Fig. (7) shows the relation between Embedment Ratio D/d and lateral capacity for single helical pile with different diameters

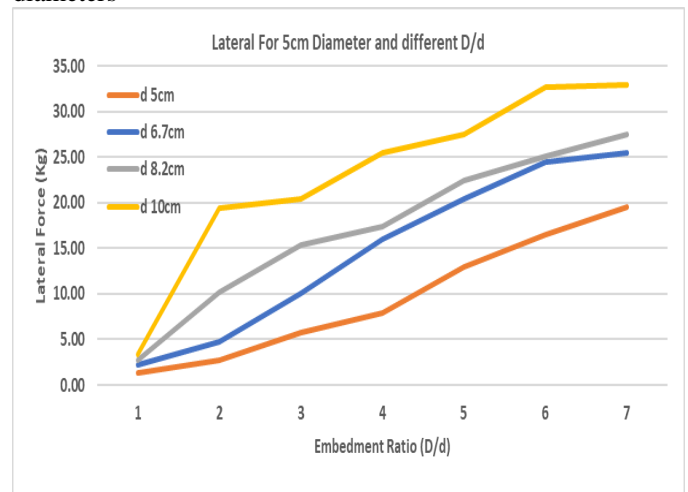


Fig. (7) Lateral capacity versus Embedment Ratio D/d for

single helical pile with different diameters

The results of compression, uplift and lateral which concluded by F.E.M are compared as following in Figs Typical compression, Uplift, Lateral loads of helical, (P_c), (P_u), (P_L), kg against embedment ratio, D/d equal to 1,2,3,4,5,6 and 7 for helix diameters, d equal 5, 6.7, 8.2 and 10 cm in sand

Fig. (8). For 5cm diameter It can be noticed the load capacities increase with increasing the embedment ratio, D/d. for the same diameter and the relationships can be represented as follows:

Fig. (8) shows the relations between compression, uplift and lateral capacities for **5 cm** Diameter and these relations can be represented by equations as follow:

$$P_c = 9.7155 (D/d) + 42.644 \quad (\text{Eq7})$$

$$P_u = 2.0321(D/d) - 1.8355 \quad (\text{Eq8})$$

$$P_L = 3.1811(D/d) - 3.1903 \quad (\text{Eq9})$$

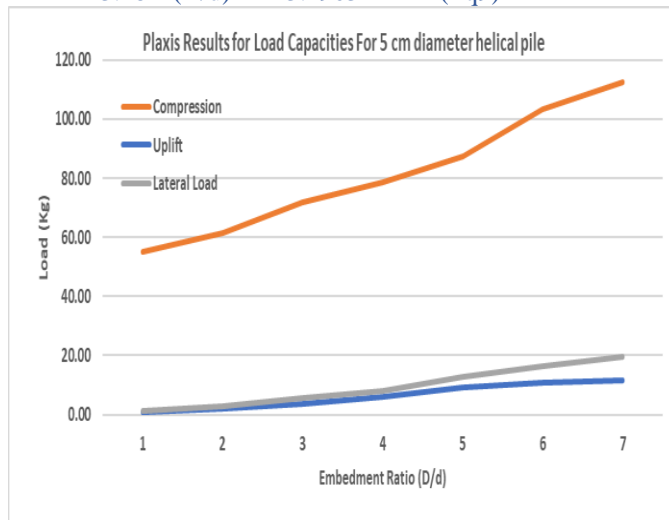


Fig. (8) Compression, Uplift and lateral capacities versus different embedment ratios for **5 cm** helical pile diameter

Fig. (9) shows the relations between compression, uplift and lateral capacities for **6.7 cm** helical pile Diameter and these relations can be represented by equations as follow:

$$P_c = 14.983 (D/d) + 91.92 \quad (\text{Eq10})$$

$$P_u = 4.2719(D/d) - 3.8021 \quad (\text{Eq11})$$

$$P_L = 4.2682(D/d) - 2.3016 \quad (\text{Eq12})$$

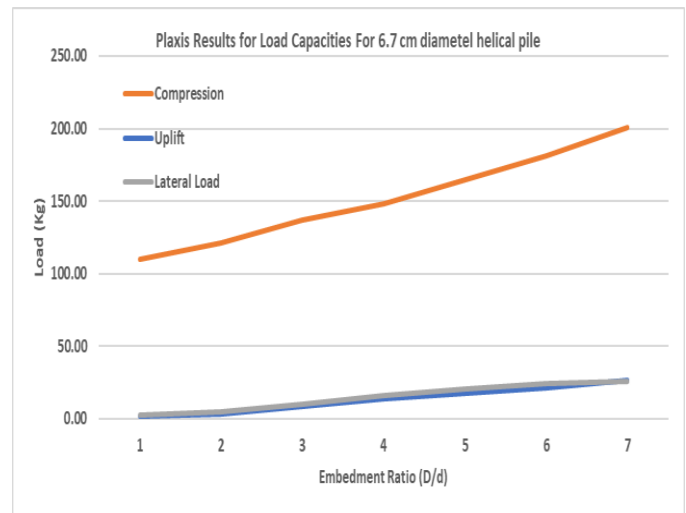


Fig. (9) Compression ,Uplift and lateral capacities versus different embedment ratios for **6.7 cm** helical pile diameter

Fig. (10) shows the relations between compression, uplift and lateral capacities for **8.2 cm** Diameter and these relations can be represented by equations as follow:

$$P_c = 21.101 (D/d) + 144.46 \quad (\text{Eq13})$$

$$P_u = 7.1599(D/d) - 6.2931 \quad (\text{Eq14})$$

$$P_L = 3.9842(D/d) + 1.2819 \quad (\text{Eq15})$$

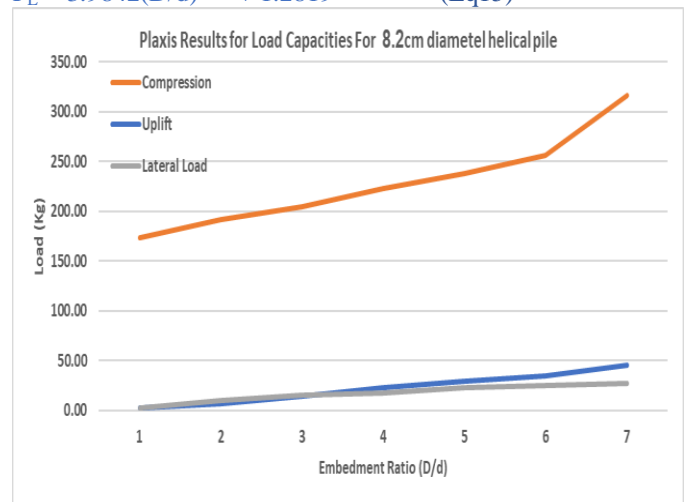


Fig.(10)) Compression ,Uplift and lateral capacities versus different embedment ratios for **8.2 cm** helical pile diameter

Fig. (11) shows the relations between compression, uplift and lateral capacities for **10 cm** helical pile Diameter and these relations can be represented by equations as follow:

$$P_c = 46.849 (D/d) + 151.27 \quad (\text{Eq16})$$

$$P_u = 14.061(D/d) - 13.722 \quad (\text{Eq17})$$

$$P_L = 4.3702(D/d) + 5.623 \quad (\text{Eq18})$$

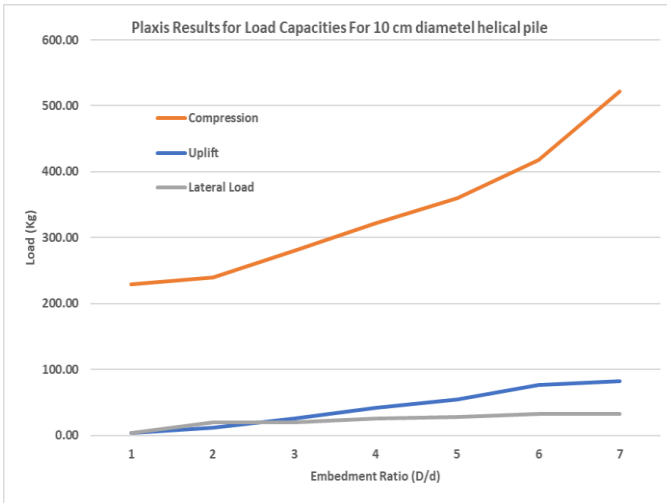


Fig. (11) Compression, Uplift and lateral capacities versus different embedment ratios for **10 cm** helical pile diameter

The experimental Results was obtained by (Walaa eldin et.al) .

it was noted from the load-Embedment ratio curves that there's a good agreement with one another of the tactic (theoretical, experimental results). Comparison between FE simulation, Theoretical and experiment ultimate load (Qu) at settlement of 10% of the helical diameter

2nd part **Comparison between Compression load Capacities for Plaxis, Theoretical and experimental Results**

Fig. (12) shows the relations between compression capacities obtained from (Plaxis, Theoretical and experimental) and embedment ratios for **5 cm** helical pile Diameter and these relations can be represented by equations as follow: $P_p = 0.3516 P_L + 35.949 = 1.799 P_T + 38.246$ (Eq19)

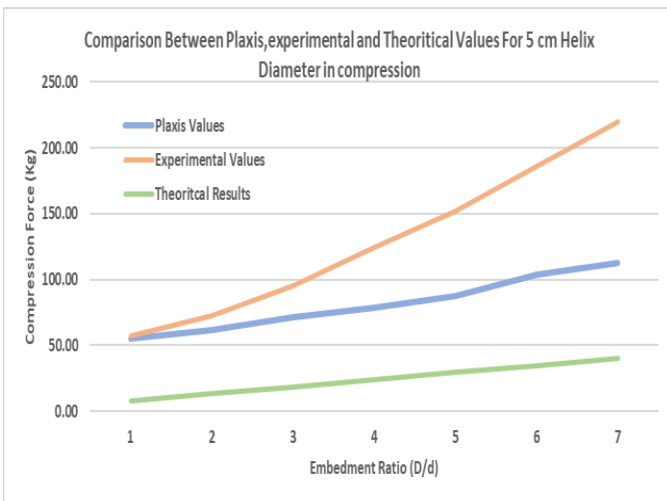


Fig. (12) Compression Force versus Embedment ratio for **5 cm** helical pile diameter for (Plaxis, Theoretical and

experimental) Results

Fig. (13) shows the relations between compression capacities obtained from (Plaxis, Theoretical and experimental) and embedment ratios for **6.7 cm** helical pile Diameter and these relations can be represented by equations as follow: $P_p = 0.347 P_L + 69.953 = 1.1643 P_T + 92.556$ (Eq20)

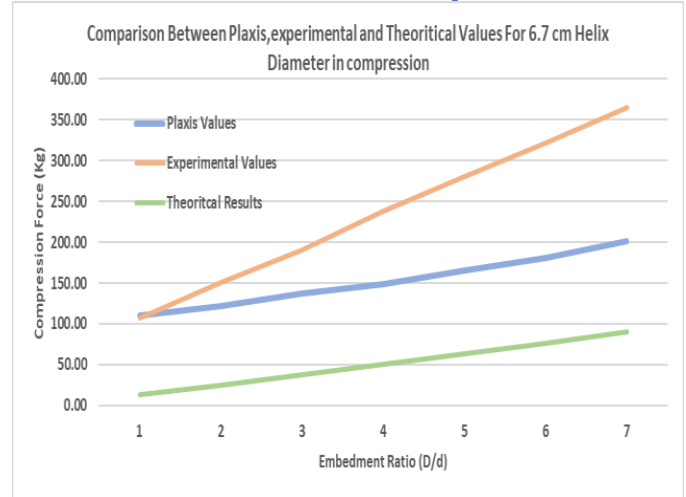


Fig. (13) Compression Force versus Embedment ratio for **6.7 cm** helical pile diameter for (Plaxis, Theoretical and experimental) Results

Fig. (14) shows the relations between compression capacities obtained from (Plaxis, Theoretical and experimental) and embedment ratios for **8.2 cm** helical pile Diameter and these relations can be represented by equations as follow: $P_p = 0.371 P_L + 110.14 = 0.8999 P_T + 145.14$ (Eq21)

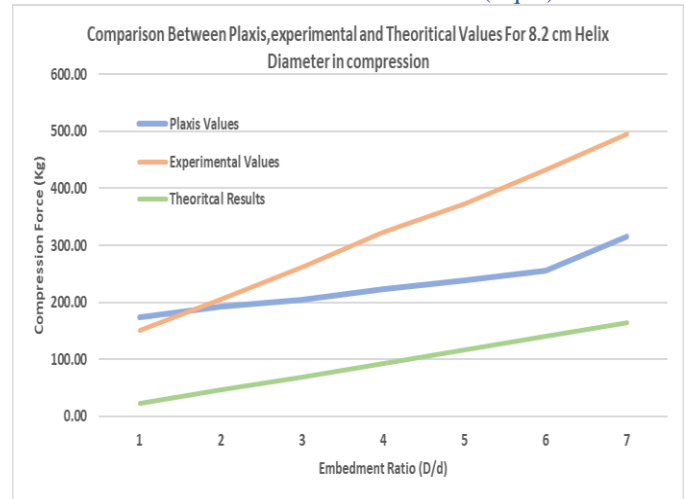


Fig. (14) Compression Force versus Embedment ratio for **8.2 cm** helical pile diameter for (Plaxis, Theoretical and experimental) Results

Fig. (15) shows the relations between compression capacities obtained from (Plaxis, Theoretical and experimental) and embedment ratios for **10 cm** helical pile Diameter and these relations can be represented by equations as follow: $P_p = 0.716 P_L + 46.117 = 1.1063$

$$P_T + 152.48$$

$$(Eq22)$$

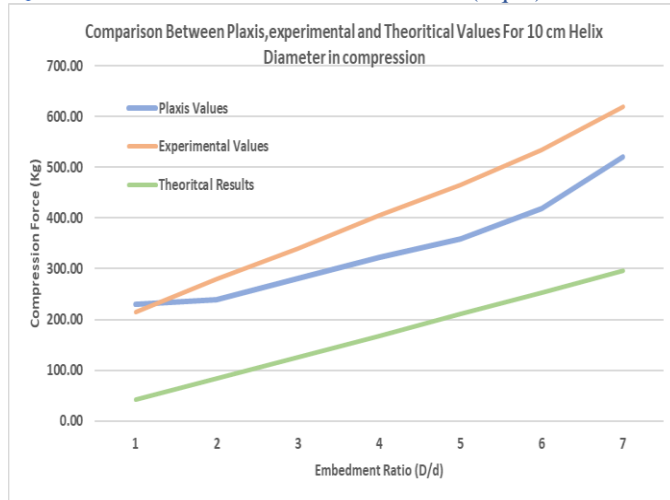


Fig.(15) Compression Force versus Embedment ratio for **10 cm** helical pile diameter for (Plaxis, Theoretical and experimental) Results

Comparison between uplift load Capacities

Fig. (16) shows the relations between uplift capacities obtained from (Plaxis, Theoretical and experimental) and embedment ratios for **5 cm** helical pile Diameter and these relations can be represented by equations as follow: $P_p = 0.9954 P_L - 0.4327 = 0.6921 P_T + 1.4795$ (Eq23)

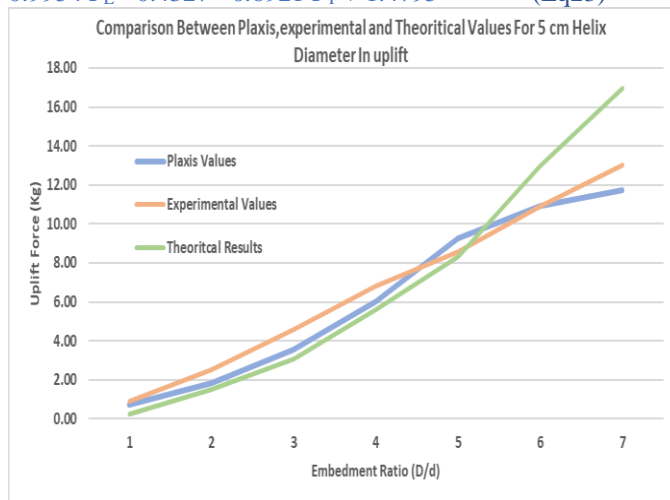


Fig. (16) Uplift Force versus Embedment ratio for **5 cm** helical pile diameter for (Plaxis, Theoretical and experimental) Results

Fig. (17) shows the relations between uplift capacities obtained from (Plaxis, Theoretical and experimental) and embedment ratios for **6.7 cm** helical pile Diameter and these relations can be represented by equations as follow: $P_p = 1.359 P_L - 0.7318 = 0.6202 P_T + 3.1069$ (Eq24)

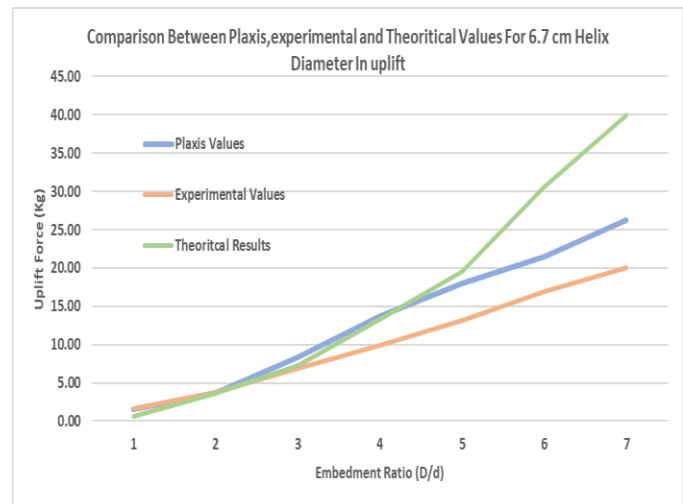


Fig. (17) Uplift Force versus Embedment ratio for **6.7 cm** helical pile diameter for (Plaxis, Theoretical and experimental) Results

Fig. (18) shows the relations between uplift capacities obtained from (Plaxis, Theoretical and experimental) and embedment ratios for **8.2 cm** helical pile Diameter and these relations can be represented by equations as follow: $P_p = 1.6494 P_L - 1.1456 = 0.5744 P_T + 5.2486$ (Eq25)

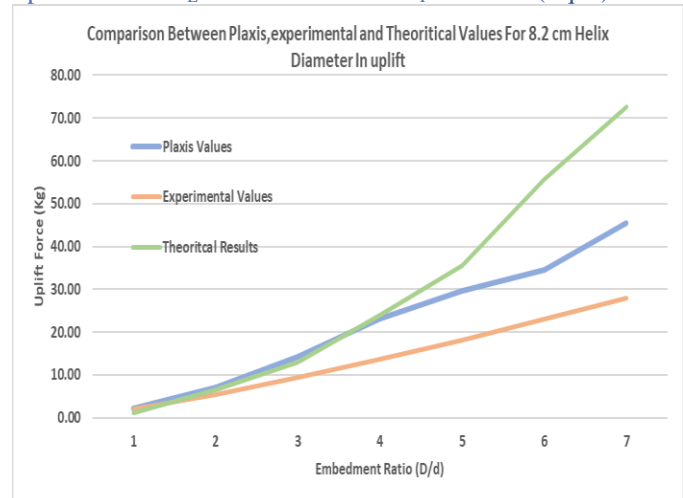


Fig. (18) Uplift Force versus Embedment ratio for **8.2 cm** helical pile diameter for (Plaxis, Theoretical and experimental) Results

Fig. (19) shows the relations between uplift capacities obtained from (Plaxis, Theoretical and experimental) and embedment ratios for **10 cm** helical pile Diameter and these relations can be represented by equations as follow: $P_p = 2.5084 P_L - 4.4569 = 0.6287 P_T + 8.8747$ (Eq26)

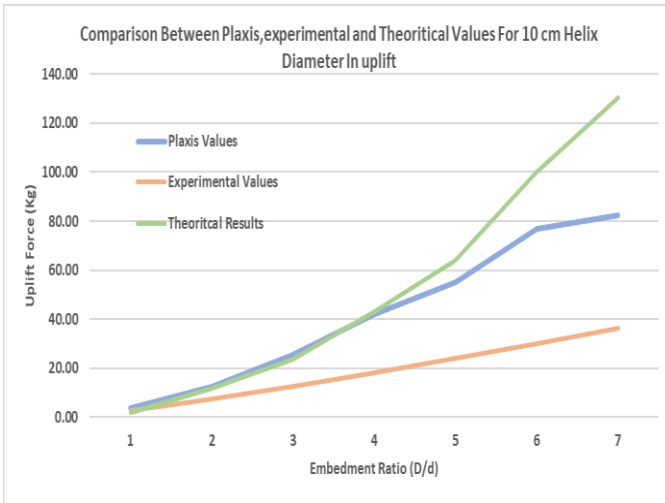


Fig. (19) Uplift Force versus Embedment ratio for **10 cm** helical pile diameter for (Plaxis, Theoretical and experimental) Results

Comparison between lateral load Capacities

Fig. (20) shows the relations between lateral capacities obtained from (Plaxis, Theoretical and experimental) and embedment ratios for **5 cm** helical pile Diameter and these relations can be represented by equations as follow: $P_p = 1.1249 P_L + 1.7646 = 2.8137 P_T + 0.5304$ (Eq27)

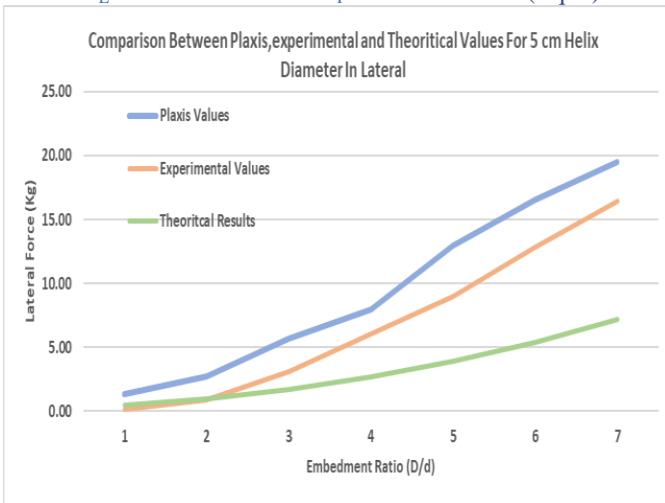


Fig. (20) lateral Force versus Embedment ratio for **5 cm** helical pile diameter for (Plaxis, Theoretical and experimental) Results

Fig. (21) shows the relations between lateral capacities obtained from (Plaxis, Theoretical and experimental) and embedment ratios For **6.7 cm** helical pile Diameter and these relations can be represented by equations as follow: $P_p = 1.2551 P_L + 3.2599 = 1.9997 P_T + 3.9301$ (Eq28)

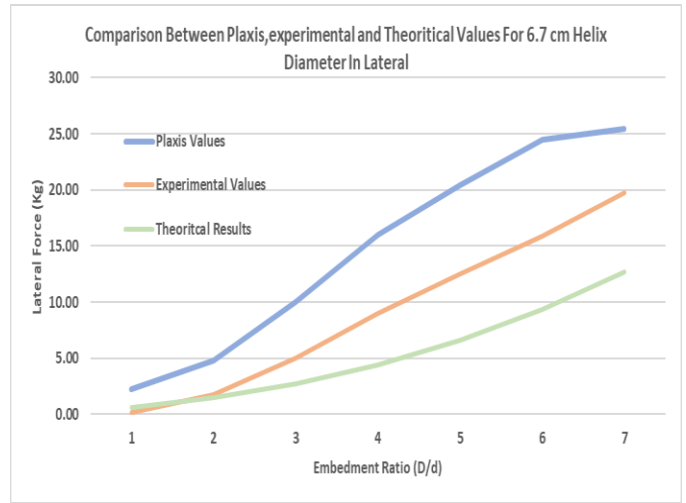


Fig. (21) lateral Force versus Embedment ratio for **6.7 cm** helical pile diameter for (Plaxis, Theoretical and experimental) Results

Fig. (22) shows the relations between lateral capacities obtained from (Plaxis, Theoretical and experimental) and embedment ratios for **8.2 cm** helical pile Diameter and these relations can be represented by equations as follow: $P_p = 1.0489 P_L + 6.4147 = 1.1972 P_T + 7.6619$ (Eq29)

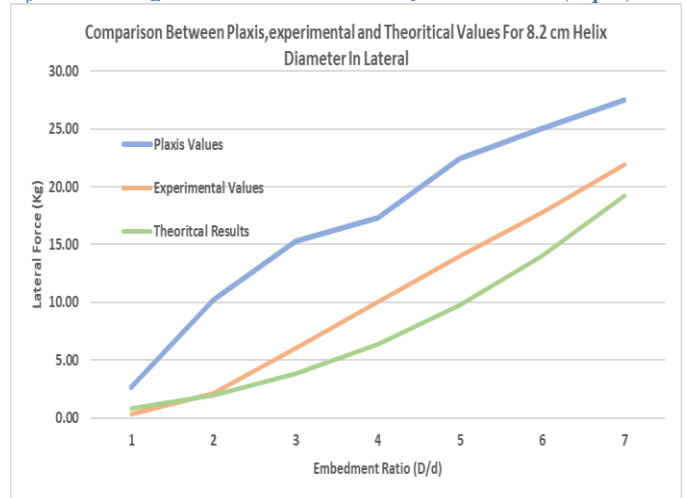


Fig. (22) lateral Force versus Embedment ratio for **8.2 cm** helical pile diameter for (Plaxis, Theoretical and experimental) Results

Fig. (23) shows the relations between lateral capacities obtained from (Plaxis, Theoretical and experimental) and embedment ratios for **10 cm** helical pile Diameter and these relations can be represented by equations as follow: $P_p = 1.0741 P_L + 10.905 = 0.8266 P_T + 13.301$ (Eq30)

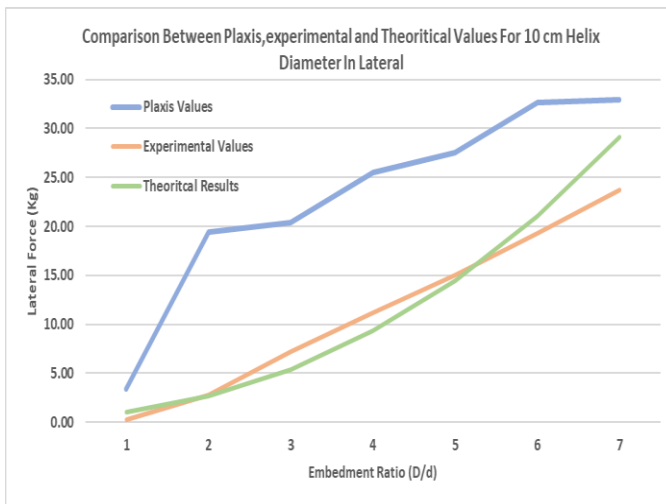


Fig. (23) lateral Force versus Embedment ratio for **10 cm** helical pile diameter for (Plaxis, Theoretical and experimental) Results

Conclusion

- 1- with the increase of helical diameter, the ultimate compression capacity increased.
- 2- with the increase of helical diameter, the ultimate uplift capacity increased.
- 3- with the increase of helical diameter, the ultimate lateral capacity increased.
- 4- with the increase of helical embedment depth, the ultimate compression capacity increased.
- 5- with the increase of helical embedment depth, the ultimate uplift capacity increased.
- 6- with the increase of helical embedment depth, the ultimate lateral capacity increased.
- 7- In compression it was found to be the experimental ultimate capacity is much higher than plaxis obtained capacities and with increasing embedment ratio the gap increase.
- 8- In compression it was found to be the theoretical ultimate capacity is approximately half the plaxis obtained and it's in a good agreement with it.
- 9- In uplift it was found to be the theoretical ultimate capacity is slightly higher than plaxis obtained capacities it's in a good agreement with it.
- 10- In uplift it was found to be the plaxis obtained ultimate capacity is slightly higher than experimental ultimate capacity it's in a good agreement with it.
- 11- In lateral it was found to be plaxis obtained ultimate capacity is 20 – 30 % higher than experimental ultimate capacity it's in a good agreement with it.

- 12- In lateral it was found to be the theoretical ultimate capacity is approximately half the plaxis obtained and it's in a good agreement with it.

References

- 1- Mitsch M.P. and Clemence S.P. (1985), "The Uplift Capacity of Helix Anchors in Sand. Uplift Behavior of Anchor Foundation in Soil ASCE, pp. 26-47.
- 2- Narasimha Rao, S., and Prasad, Y.V., (1991), "Estimation of Uplift Capacity of Helical Anchors in Clays", ASCE, Journal of Geotechnical Engineering Division, Vol. (199), pp. 352–357.
- 3- Zhang, D. (1999). "Predicting capacity of helical screw piles in Alberta soils". MSc Thesis, Dept. of Civil and Environmental Engineering, University of Alberta, Edmonton, Alberta, 304 p.
- 4- El-Naggar, M.H., and Livneh, B., (2008), "Axial Testing and Numerical Modeling of Square Shaft Helical Piles under Compressive and Tensile Loading", Canadian Geotechnical Journal, Vol. (45), pp.1142–1155.
- 5- M. Sakr (2011). Installation and performance characteristics of high capacity helical piles in cohesionless soils. DFI Journal – The Journal of the Deep Foundations Institute, 2011, vol. 5, no. 1, 39-57
- 6- S. Mittal, B. Ganjoo, S. Shekhar.(2010) , "Static equilibrium of screw anchor pile under lateral load in sand", Geotech. Geol. Eng. 28 (2010) 717–725.
- 7- Abdel-Rahim, Hamdy HA, Yehia Kamal Taha, and Walla El din El sharif Mohamed(2013). "The compression and uplift bearing capacities of helical piles in cohesionless soil." Journal of Engineering Sciences 41, no. 6 (2013): 2055-2064.
- 8- in cohesionless soil, pp. 2055 – 2064

Notations

- A = surface area of the helix plate, cm² ;
d = helix plate diameter, cm ;D =embedded depth of helix in sand, cm;
D/d = embedment ratio;
P_c = Bearing capacity (compression load) of helix pile, kg;
P_u= Bearing capacity (uplift load)of helix pile, kg;
P_c = Compression Force;
P_u = Uplift Force;
P_L = Lateral Force;
P_p = Plaxis calculated Force;
P_L = lab determined Force;
P_T = Theoretical Calculated force